



# Synthesis and Characterization of Robust SiO<sub>2</sub>-Phase Change Materials (PCM) Microcapsules

Jinliang An,<sup>1,2,3,4</sup> En-Hua Yang,<sup>5,\*</sup> Fei Duan,<sup>4</sup> Yong Xiang<sup>2,\*</sup> and Jinglei Yang<sup>3,6\*</sup>

## Abstract

Inorganic SiO<sub>2</sub> microencapsulated phase change materials (MEPCMs) have been developed via polymerization reaction and electrostatic interaction in an emulsion system. The resultant microcapsules were systematically characterized in terms of morphology, composition, thermal stability, durability and mechanical property. The energy storage capacity of the obtained microcapsules ranges from 190.5 J/g to 225.5 J/g (pure octadecane: 250.6 J/g) when the core material is octadecane at different sizes. SiO<sub>2</sub>-PCM microcapsules showed improved energy storage efficiency in terms of shorter melting and freezing durations attributed by the higher thermal conductivity of inorganic silica shell compared with that of polymer shell encapsulated PCM. Repeatable melting and freezing processes after 150 cycles revealed excellent shell tightness and thermal stability of the resultant microcapsules. The high apparent compressive strength of individual SiO<sub>2</sub>-PCM microcapsule indicated good survivability in further materials processing for energy storage. The robust SiO<sub>2</sub>-PCM microcapsules obtained from a facile fabrication approach in this study have great potential applications for developing energy efficient materials.

**Keywords:** Silica shell; Phase change material microcapsules; Energy storage capacity; Energy storage efficiency; Robustness.

Received: 30 August 2020; Accepted: 22 May 2021.

Article type: Research article.

## 1. Introduction

With the increasing demand on energy, there is an urgent need to identify renewable energy sources and to invent novel materials for energy storage.<sup>[1,2]</sup> Latent heat storage of phase change material (PCM) achieved via a solid-liquid phase transition is a promising technology. With large latent heat storage capacity and narrow operating temperature range, PCMs provide an efficient way to store thermal energy. PCMs have been widely used in smart textiles to regulate body

temperature, in heat transfer media to save energy, and in solar energy devices for energy storage.<sup>[3,4]</sup> Organic PCMs have attracted great attention due to their excellent phase change performance. Among them, N-alkanes (*i.e.* paraffin waxes) are the most promising organic PCMs because they are chemically inert with low vapor pressure, ecologically harmless, noncorrosive, cheap, and widely available. Owing to these desirable characteristics, N-alkanes have been used in various applications.<sup>[1,5-7]</sup> Octadecane is an alkane hydrocarbon with a phase change temperature of around 26–28 °C and a high latent heat capacity of 241.2 J/g.<sup>[8]</sup> Since the phase change temperature of octadecane is in the thermal comfort range of human body, octadecane has been used in garments and building products.<sup>[5,6,9-12]</sup>

However, direct incorporation of bulk PCM into a matrix such as textile or gypsum wall board is difficult due to leaking of PCM during solid-liquid phase change. Packaging of bulk PCM is therefore often necessary so that melting and solidification process is accomplished in a container which prevents leaking of PCM. In addition, packaged PCM should be compatible mechanically and chemically with the surrounding matrix, possesses a stable structure during phase change, and provides sufficient surface area to encourage heat transfer. Microencapsulation of PCM is there an arrestive way for PCM packaging. Many studies reported encapsulation of

<sup>1</sup> School of Civil Engineering, Hebei University of Engineering, Handan, Hebei 056038, China.

<sup>2</sup> School of Materials and Energy, University of Electronic Science and Technology of China, Chengdu, Sichuan 611731, China.

<sup>3</sup> Center for Engineering Materials and Reliability, HKUST Fok Ying Tung Research Institute, Guangzhou, Guangdong 511458, China.

<sup>4</sup> School of Mechanical and Aerospace Engineering, Nanyang Technological University, Singapore 639798.

<sup>5</sup> School of Civil and Environmental Engineering, Nanyang Technological University, Singapore 639798.

<sup>6</sup> Department of Mechanical and Aerospace Engineering, Hong Kong University of Science and Technology, Kowloon, Hong Kong SAR, China.

\* Email: [ehyang@ntu.edu.sg](mailto:ehyang@ntu.edu.sg) (E. Yang), [xyg@uestc.edu.cn](mailto:xyg@uestc.edu.cn) (Y. Xiang), [maeyang@ust.hk](mailto:maeyang@ust.hk) (J. Yang)

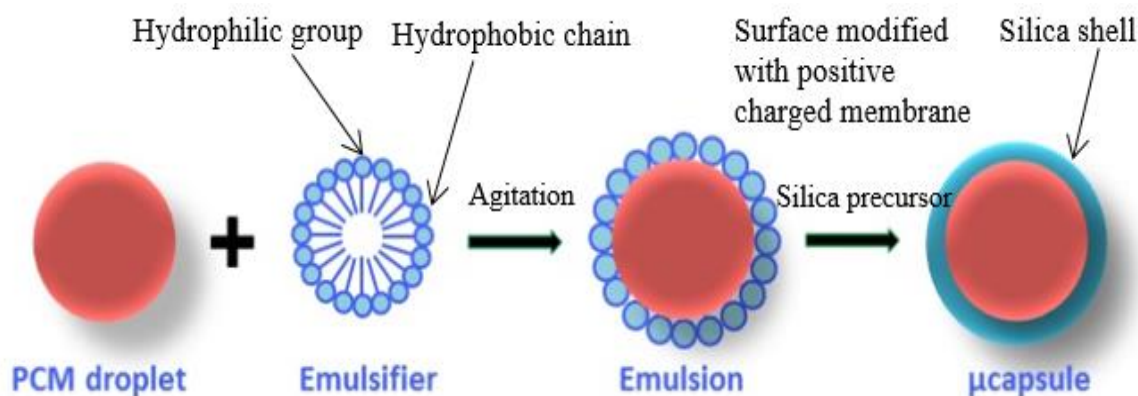


**Fig. 1** Schematic process of microencapsulation of PCM via deposition of hydrolyzed  $\text{SiO}_2$  precursor.

PCM with organic shell such as poly-urea, polyurethane and poly-urea formaldehyde.<sup>[13-15]</sup> Wang and Zhang<sup>[16]</sup> synthesized the microencapsulated octadecane PCM with polyurea shell via interfacial polymerization. Li *et al.*<sup>[17]</sup> prepared a kind of formaldehyde shell containing PCMs. The organic shell, however, has some major disadvantages including high flammability, poor thermal and chemical stability, and low thermal conductivity. To overcome these shortcomings, PCM encapsulated with inorganic silica shell was synthesized in oil in water (O/W) emulsion system<sup>[11-14]</sup> via a sol-gel method<sup>[18,19]</sup>, was currently reported. However, durability of reported microcapsules is discontented in most of current studies<sup>[9-11]</sup>, *i.e.* thermal stability of microcapsules changes significantly after multiple cooling-heating cycles treated. In addition, an essential property, compressive strength of individual silica-PCM microcapsule, has not been investigated in any articles till now. It is known that high strength of microcapsule can protect core PCM from external force to ensure no variation of latent heat storage capacity, which makes capsules more practical for real application.

In this study, a new facile approach to synthesize  $\text{SiO}_2$ -PCM microcapsules was developed to address the reported issues as shown in Fig. 1, such as poor thermal stability and weak mechanical strength. Four innovative methods are proposed in this study. First, it is based on the principle of electrostatic adsorption that  $\text{Si}(\text{OH})_4$  monomer is adsorbed on polyurea (PUA) membrane, and then it is further polymerized to produce inorganic silica shell; second, the outer surface of PCM capsule is a micro-nano hierarchical structure with a larger specific surface area, which is more conducive to the heat exchange of the core PCM; third, the compressive strength test of a single PCM microcapsule is proposed for the first time; finally, the thermal stability of the PCM microcapsule is excellent, the heat enthalpy is basically unchanged after 150 heating and cooling cycles.

In conclusion, a special double layer structure with inner polyurea membrane and outer silica shell was innovated and optimized after parametric study.<sup>[20]</sup> The resultant  $\text{SiO}_2$ -PCM microcapsules were systematically characterized and analyzed in terms of heat storage capacity and efficiency, thermal stability, and mechanical strength.

## 2. Materials and experiments

### 2.1 Materials and synthesis of $\text{SiO}_2$ -PCM microcapsules

Chemicals including arabic gum, hexamethylene diisocyanate (HDI), polyethylenimine (PEI, Mw~1300), hexane, octadecane, trimethoxymethylsilane (MTTS) and hydrochloric acid solution (HCl, 0.1N) were purchased from Sigma Aldrich and used directly without further purification.

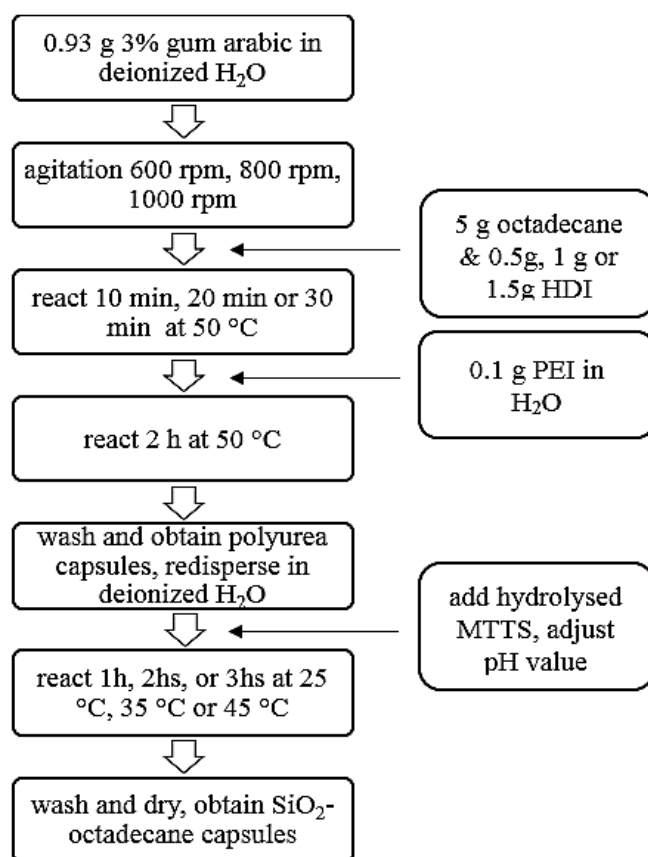


**Fig. 2** Schematic diagram of synthesis of silica-octadecane microcapsules.

As shown in Fig. 2, at ambient temperature, 30 ml of deionized water and 0.93 g of 3 wt.% aqueous solution of arabic gum were mixed in a 200 ml beaker. The beaker was suspended in a temperature-controlled water bath on a programmable hot plate with an external temperature probe.

The solution was agitated at 600-1000 rpm with a digital mixer (Caframo) driving a three-bladed propeller. The solution was heated to 50 °C at a heating rate of 5 °C/min. 5 g octadecane and 0.5-1.5 g HDI were then mixed together and slowly added into the aqueous solution to generate emulsion for 10-30 min. After that, 10 g of 1 wt.% aqueous solution of PEI was added drop wise into the emulsion system. After 2 hours continuous agitation, both the stirrer and hot plate were switched off. The resultant PUA-PCM pre-capsules (octadecane core with a thin layer of polyurea membrane) were washed with distilled water for three times. After that, the PUA-PCM pre-capsules were re-dispersed into beaker loaded with 30 ml deionized water. MTTs was added into 4 ml aqueous solution (pH=3, prepared using 0.1N HCl) and agitated to initiate hydrolysis at 35 °C for 1 hr. Subsequently, the pre-hydrolyzed MTTs was slowly added into the solution containing PUA-PCM pre-capsules and the solution was agitated at 150 rpm for 1-3 h at certain temperature (25, 35, or 45 °C) to allow complete deposition of silica on the surface of PUA-PCM pre-capsules through electrostatic interaction. The resultant SiO<sub>2</sub>-PCM microcapsules were washed with deionized water and collected after air-drying at room temperature in the fume hood for 24 hours before further analysis.

## 2.2 Characterizations

Morphology and shell thickness of microcapsules were observed using field-emission scanning electron microscope (FE-SEM, JEOL, JSM-7600F) equipped with energy dispersive X-ray spectroscopy (EDS). EDS was used to probe the chemical composition of the shell material. To prepare the sample, small amount of microcapsules was distributed uniformly on a conductive adhesive tape. Few capsules were ruptured by a razor blade in order to observe core-shell structure. The sample was sputter coated with gold for 40-50 seconds in vacuum environment and taken out for further analysis.

Fourier transform infrared spectroscopy (FTIR, Varian 3100) was engaged to distinguish the constituents of the SiO<sub>2</sub>-PCM microcapsules, octadecane (core material), and the shell. To obtain the shell material, capsule samples were crushed thoroughly and washed three times with hexane to remove core material (octadecane). After that, the residue (*i.e.* shell material) was filtered and dried in fume hood at room temperature for 3 hours.

Thermal gravimetric analysis (TGA, Q2950, TA Instruments) and differential scanning calorimetry (DSC, Q200, TA Instruments) were carried out to evaluate the thermal properties of the capsules. TGA on the SiO<sub>2</sub>-PCM capsules, octadecane, and the shell were conducted in nitrogen atmosphere to evaluate the weight change of sample as a function of increasing temperature up to 600 °C with a constant heating rate of 10 °C/min. Isothermal TGA test on the SiO<sub>2</sub>-PCM capsules and octadecane were carried out in nitrogen atmosphere at 80 °C for 1 hour to evaluate thermal stability of sample as a function of time. DSC on the SiO<sub>2</sub>-

PCM capsules, the PUA-PCM pre-capsules, and octadecane were evaluated in N<sub>2</sub> atmosphere with a heating/cooling rate of 10 °C/min. Encapsulation ratio (*R*) and thermal storage capacity ( $\phi$ ) of microcapsules can be determined from the following equations.<sup>[21,22]</sup>

$$R (\%) = \frac{\Delta H_{m,capsule}}{\Delta H_{m,PCM}} \times 100 \quad (1)$$

$$\phi (\%) = \frac{(\Delta H_{m,capsule} + \Delta H_{c,capsule})/R}{\Delta H_{m,PCM} + \Delta H_{c,PCM}} \times 100 \quad (2)$$

where  $\Delta H_{m,capsule}$  and  $\Delta H_{c,capsule}$  in J/g are the melting and solidification enthalpy of capsules, respectively. Similarly  $\Delta H_{m,PCM}$  and  $\Delta H_{c,PCM}$  in J/g are the melting and solidification enthalpy of octadecane, respectively. Enthalpy was calculated by integrating the area under the DSC curve using TA Universal Analysis software. Furthermore, to evaluate the stability and reliability, SiO<sub>2</sub>-PCM capsules were undergone 150 heating and cooling cycles in DSC.

Core fraction was obtained by comparing the weight change before and after removing the core material from the microcapsules. Few grams of SiO<sub>2</sub>-PCM capsules were collected and weighted first,  $W_{capsule}$  in g. The capsule samples were crushed thoroughly and washed three times with hexane to remove core material (octadecane). After that, the residue (*i.e.* shell material) was filtered and dried in fume hood at room temperature for 3 hours. The weight of the shell material,  $W_{shell}$  in g, was measured and recorded. Core fraction (%) can be calculated with the following Equation. 3. Core fraction of each sample was measured 3 times and the average and standard deviation were reported.

$$Core\ fraction (\%) = \frac{W_{capsule} - W_{shell}}{W_{capsule}} \times 100 \quad (3)$$

Mechanical strength of individual capsule with liquid core material was tested under compression with a program-controlled stepper actuator (Physik Instrument M-230S) at a loading rate of 2  $\mu$ m/s.<sup>[28]</sup> A 0.5 N load cell (FUTEK) was used to record the compressive load. Since octadecane with a phase change temperature of 28-30 °C is in solid state at room temperature (22 °C), microcapsules were heated first to 100 °C for 10 min to ensure the core material remaining liquid during the compression test. Apparent mechanical strength of individual capsule under compression,  $\sigma_c$  in MPa, was estimated using Eqn. 4:<sup>[23]</sup>

$$\sigma_c = \frac{P_{max}}{\pi \left( \left( \frac{D_o}{2} \right)^2 - \left( \frac{D_i}{2} \right)^2 \right)} = \frac{4P_{max}}{\pi (2D_o - t)t} \quad (4)$$

where  $P_{max}$  in N is the peak load,  $D_o$  and  $D_i$  in  $\mu$ m are the outer and inner diameter of capsule, respectively, and  $t$  in  $\mu$ m is the shell thickness.

## 3. Results and discussion

### 3.1 Mechanism of formation of silica-PCM capsules

In this study, the resultant silica PCM capsules were prepared based on oil-in-water emulsion system. As can be seen in Fig. 1. Liquid PCM together with HDI as the oil phase is introduced into aqueous solution containing surfactant. Under agitation, stable oil droplets are formed due to the function of surfactant. PEI aqueous solution is then added drop wise.

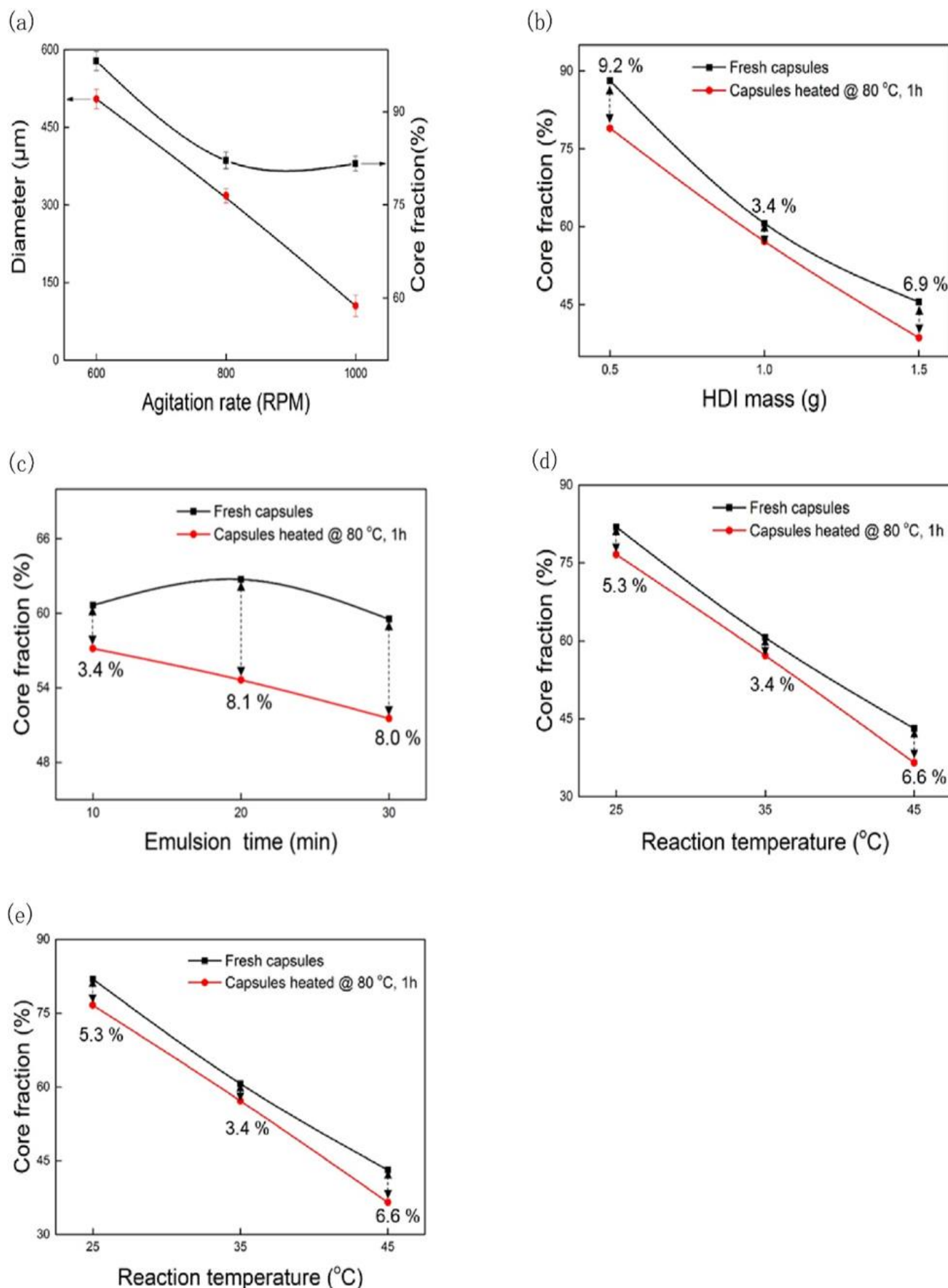


**Fig. 3** Diameter and core fraction of  $\text{SiO}_2$ -PCM capsules as functions of (a) agitation rate; and core fraction and thermal stability of  $\text{SiO}_2$ -PCM capsules as functions of (b) HDI mass, (c) emulsion time, (d) reaction temperature, and (e) reaction time.



**Table 1.** DSC thermal properties of octadecane and SiO<sub>2</sub>-PCM capsules with different sizes.

Sample	Melting process		Solidification process		Encapsulation ratio (%)	Thermal storage capacity (%)
	T <sub>m</sub> (°C)	ΔH <sub>m</sub> (J g <sup>-1</sup> )	T <sub>c</sub> (°C)	ΔH <sub>c</sub> (J g <sup>-1</sup> )		
Octadecane	27.1	250.6	27.0	227.9	-	-
SiO <sub>2</sub> -PCM capsule@100μm	27.3	210.2	26.9	188.1	83.9	99.2
SiO <sub>2</sub> -PCM capsules@300μm	27.4	223.5	27.1	202.3	89.2	99.8
SiO <sub>2</sub> -PCM capsules@500μm	27.5	230.3	27.1	208.1	91.9	99.7

Note: T<sub>m</sub> and T<sub>c</sub> are melting and solidification temperatures, respectively. ΔH<sub>m</sub> and ΔH<sub>c</sub> are melting and solidification enthalpies, respectively.

Temperature is set as 50 °C to initiate the reaction between HDI and PEI for 2 hours. During this process, positively charged polyurea (PUA) membrane is formed around the droplets (*i.e.*, PUA pre-capsules). It is known that PEI molecules contain long-chain of NH<sub>2</sub> group which is positively charged in aqueous solution. Therefore, negatively charged pre-hydrolysis of MTTs (Si(OH)<sub>4</sub> monomer) tends to be attracted on PUA membrane by means of electrostatic interaction.<sup>[24,25]</sup> Adjusting the pH of above solution to 3.0 and extending the reaction for a certain time at ambient temperature, dense and solid silica shell begins to form and grow. Finally well-defined and complete silica shell is obtained.

Fundamentally, the formation of silica shell relies on the deposition of MTTs precursor on the surface of PUA membrane via electrostatic force because negatively charged monomer Si(OH)<sub>4</sub> has the tendency to be attracted by and deposits on the positively charged polyurea surface which further forms Si-O-Si (*i.e.* silica) network structure. A fine balance between hydrolysis and condensation of MTTs precursor is necessary to ensure a well-defined core-shell structure of the SiO<sub>2</sub>-PCM microcapsules. The properties of resultant capsules were significantly affected by the synthesis conditions such as agitation rate. Specifically, proper pre-hydrolysis of MTTs and pH value play significant roles in the formation of silica shell. A suitable acidic condition is beneficial for the hydrolysis of MTTs, resulting in accelerating the hydrolysis rate of MTTs. Meanwhile the condensation rate of hydrolyzed monomer is inhibited.<sup>[21]</sup>

### 3.2 Parametric study

Five key factors, including agitation speed (600-1000 rpm), HDI dosage (0.5-1.5 g), emulsion time (10-30 mins), reaction temperature (25-45 °C), and reaction time (1 hour-3 hours), were systematically studied to reveal their influence on core fraction and thermal stability of the resultant SiO<sub>2</sub>-PCM microcapsules. Reference synthesis conditions are agitation speed of 900 rpm, HDI dosage of 1 g, emulsion time of 10 min, reaction temperature of 35 °C, and reaction time of 3 hours.

Only one factor is changed every time and the other factors remain as the reference synthesis conditions.

Fig. 3a shows the diameter and core fraction of SiO<sub>2</sub>-PCM capsules under different agitation rate. As can be seen, the size of the microcapsules decreases from 500 μm to 100 μm and the core fraction reduces from 89.5 wt.% to 75.9 wt.% when the agitation speed increases from 600 rpm to 1000 rpm, respectively. It reveals that core content of capsules was increased with capsule size enlarged. Probably, it is ascribed to lower specific surface area of larger capsules, resulting in less quantity of Si(OH)<sub>4</sub> monomer deposited on capsule surface.

In addition, encapsulation ratio can be obtained based on the enthalpy of SiO<sub>2</sub>-PCM capsules.<sup>[26]</sup> In which enthalpy calculated from DSC, it is known that silica is not phase change material. Therefore, the total enthalpy of SiO<sub>2</sub>-PCM capsules is attributed to core PCM. Table 1 gives the enthalpy of samples and their corresponding encapsulation ratio. It shows that encapsulation ratio increased from 83.9 wt.% to 91.9 wt.% when capsule diameter increased from 100 μm to 500 μm. In addition, a physical experiment was carried out to validate the results obtained through enthalpy method. As shown in Fig. 3a, it shows the core fraction increased from 75.9 wt.% to 89.5 wt.%, when diameter of capsules increased from 100 μm, 300 μm and 500 μm. Comparing these two results obtained from two different approaches, it indicates that calculation of enthalpy approach shows good agree with experimental results.

It is well known that latent heat can only be storied by core PCM instead of silica shell. Hence, the content of core PCM is the only factor dominate encapsulation ratio. Thermal storage capacity stands for service efficiency of PCM during phase change process. Normally, encapsulation ratio and thermal storage capacity are used to characterize the phase change performance, and phase change enthalpy has a heavily relationship with encapsulation ratio (R) and thermal storage capacity (φ) of silica-PCM capsules. Based on the equation (1), theoretical encapsulation ratio and thermal storage capacity can be obtained as listed in Table 1. In which the highest

encapsulation ratio of silica-PCM capsules is about 91.9 wt.% at diameter 500  $\mu\text{m}$ , this value is approximately equivalent to the data 89.5 wt.% at the same size investigated by practical experiment as shown in Fig. 3a. These two comparable approaches demonstrate that of silica-PCM capsules have a high encapsulation ratio at a proper capsule size obtained by regulating agitation rate, indicating that high latent heat storage capacity of silica-PCM capsules can be obtained successfully. Similarly, thermal storage capacity can be calculated using equation (2), all of the thermal storage capacity of capsules are higher than 99%, meaning that almost all of the encapsulated core PCM are functional and active for thermal storage.

Fig. 3b reveals that the core fraction of  $\text{SiO}_2$ -PCM microcapsule reduces significantly from 88.1 to 45.5 wt.% as the HDI amount increases from 0.5 to 1.5 g. This phenomenon is because HDI mixed with PCM as the core materials, PCM mass is a constant 5 g, when HDI mass increased from 0.5 g to 1.5 g, the percentage of PCM (core materials: PCM&HDI) is decreased gradually. Capsules synthesized with 1 g HDI exhibits best thermal stability with only 3.4 % loss in weight, followed by capsules synthesized with 1.5 g HDI (6.9 % weight loss) and with 0.5 g HDI (9.2 % weight loss), after 1 h isothermal heating at 80  $^{\circ}\text{C}$ . The optimal HDI dosage of 1 g in current study allows the formation of positively charged polyurea membrane capsules, enhances deposition of nano-silica particles, and forms dense silica shell. At lower dosage of HDI, formation of positively charged polyurea membrane capsules is hindered and deposition of nano-silica particles is limited, resulting in loose shell structure and low thermal stability. When higher HDI is used, surrounding water molecular can diffuse into the capsule, react with excessive HDI to form polyurea inner shell, and simultaneously generate carbon dioxide which can cause porous and loose shell structure, resulting in reduction of thermal stability of capsules.

As shown in Fig. 3c, core fraction of capsules remains largely the same at different emulsion time with a core fraction around 62 wt.%. Furthermore, thermal stability of capsules decreases with increasing emulsion duration as 3.4 wt.% weight loss was observed for the capsules subject to 10 min emulsion while 8 wt.% weight loss was registered for the capsules subject to 30 min emulsion. This may be ascribed to consumption of HDI due to reaction with water molecular at prolonged emulsion duration, resulting in insufficient amount of HDI to reaction with PEI to form positively charged polyurea membrane. Therefore, deposition of  $\text{Si}(\text{OH})_4$  monomer and formation of tight silica shell are restricted.

Influence of reaction temperature on core fraction and thermal stability is shown in Fig. 3d. As can be seen, core fraction of capsules reduces significantly from 81.9 to 43.1 wt.% when the reaction temperature increases from room temperature (25  $^{\circ}\text{C}$ ) to 45  $^{\circ}\text{C}$ . This may be attributed to balanced reaction between hydrolysis and condensation of MTTs, deposition of  $\text{Si}(\text{OH})_4$  monomers on capsule surface are encouraged. At higher temperature, condensation of

$\text{Si}(\text{OH})_4$  monomers performs more quickly to generate silica shell, resulting in the content of silica shell increased in the capsules, *i.e.* core fraction of capsules under 45  $^{\circ}\text{C}$  about 43.1 wt.% is the lowest one among these three. The resultant capsules under 35  $^{\circ}\text{C}$  reaction temperature maintained at 80  $^{\circ}\text{C}$  for 1 h, the release of core octadecane was only about 3.4 wt.%. However, for capsules synthesized under reaction temperature of 25  $^{\circ}\text{C}$  and 45  $^{\circ}\text{C}$ , the release of core octadecane were 5.3 wt.% and 6.6 wt.%, respectively. Generally, a proper reaction temperature could promote the formation of silica shell. Herein resultant capsules under reaction temperature of 35  $^{\circ}\text{C}$  performed the best thermal stability. Under this circumstance, the hydrolysis product of MTTs sufficiently absorbed on capsule surface via electrostatic interaction. Gradually, tight and stiff structure of silica capsule shell formed, which efficiently protected the leakage of core octadecane. However, the formation of shell structure appeared loosely and defectively under the unsuitable reaction temperature of 25  $^{\circ}\text{C}$  and 45  $^{\circ}\text{C}$ , resulting in higher release ratio of core octadecane under isothermal at 80  $^{\circ}\text{C}$  for 1 hour. It demonstrates that the hydrolysis and condensation of MTTs were more sensitive for the system temperature.

The influence of reaction time of 1 hour, 2 hours, and 3 hours on the resultant capsules was investigated and evaluated by core fraction and thermal resistance of capsules. As can be seen in Fig. 3e, the core fraction of capsules reduced from 90.1 to 60.7 wt.% when reaction time was prolonged from 1 hour to 3 hours. It can be explained that a large quantity of silica deposited on the capsule surface with the reaction time increased from 1 hour to 3 hours. And thicker shell wall formed by silica resulting in reduction of core fraction. Core fraction of capsules decreased about 10.3 wt.% after isothermal at 80  $^{\circ}\text{C}$  for 1 hour when reaction duration was 1 hour. When reaction time increased to 2 hours, the release of core octadecane about 4.2 wt.% at the same condition. Subsequently, reaction time was extended to 3 hours, core fraction of capsules decreased only about 3.4 wt.% after isothermal at 80  $^{\circ}\text{C}$  for 1 hour. This good thermal resistance phenomenon was ascribed to the denser shell wall structure of capsules to decrease the evaporation of core PCM. Therefore, the optimal capsules can be obtained when reaction duration was 3 hours.

### 3.3 Morphology and physical properties of $\text{SiO}_2$ -PCM microcapsules

A digital image of  $\text{SiO}_2$ -PCM microcapsules is shown in Fig. 4a, which appears like white powder. And it is made of  $\text{SiO}_2$ . As can be seen in Fig. 4b, it presents the EDS spectra probed from the surface of the microcapsules. The inset table in Fig. 4b reveals high quantity of Si and O elements suggesting successful deposition of silica as the shell material.

In order to observe microstructure of capsules clearly, SEM was introduced as can be seen in Fig. 4c. The capsules are in spherical shapes with a diameter of about  $200 \pm 15 \mu\text{m}$  (estimated using Software ImageJ to count at least 100 sample

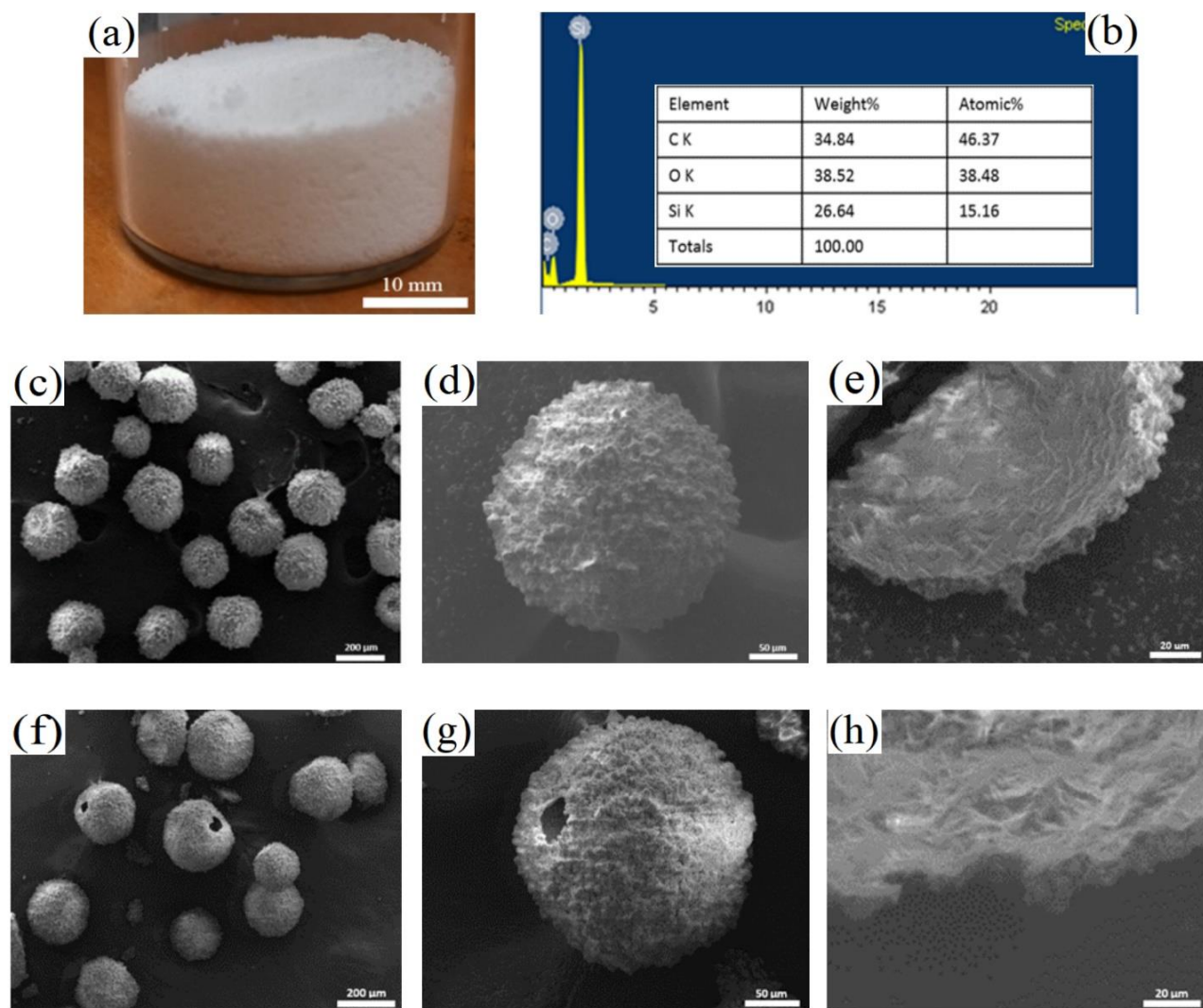


**Fig. 4** Digital photograph of (a) SiO<sub>2</sub>-PCM capsules and (b) EDS of SiO<sub>2</sub>-PCM capsules; and SEM images of SiO<sub>2</sub>-PCM microcapsules: (c) overview of SiO<sub>2</sub>-PCM capsules, (d) individual microcapsule, (e) shell profile, (f) overview of sintered SiO<sub>2</sub>-PCM capsules, (g) sintered individual microcapsule, and (h) sintered shell profile.

capsules). The surface of the capsule presents coarsely which may be ascribed to random deposition of silica precursor and thus forming rough surface with protruding nubs-like morphology (Fig. 4d). Well-defined core-shell structure with a very dense shell of about 10  $\mu\text{m}$  in thickness without any defects can be observed in Fig. 4e.

To check the strength and stability of the silica shell, Fig. 4f shows the morphology of sintered SiO<sub>2</sub>-PCM microcapsules. It reveals that most of the heat-treated microcapsules are still in spherical shape. However, few micro-holes appear on the shell due to evaporation of PCM during sintering process (Fig. 4g). Shell thickness of sintered capsules remains unchanged at approximate 10  $\mu\text{m}$  (Fig 4h) which indicates that pristine capsule shell almost consists of inorganic silica.

In order to verify that PCM is successfully microencapsulated, the core and shell materials are only physically bonded without chemical reaction, FTIR spectra was used to characterize different bond of shell material, octadecane (core material), and SiO<sub>2</sub>-PCM capsules are shown

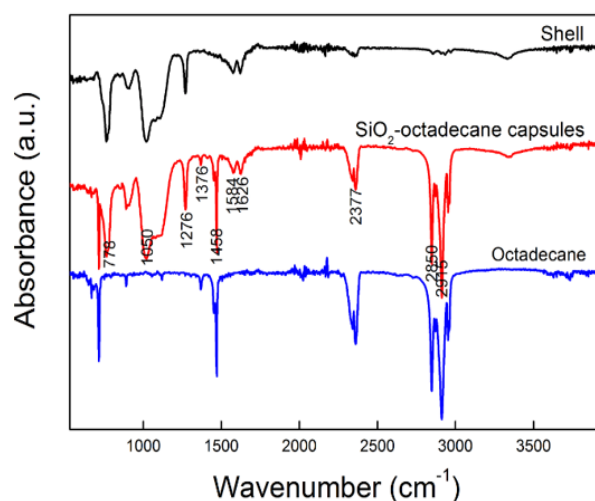


**Fig. 5** FTIR spectra of shell, SiO<sub>2</sub>-PCM capsules, and octadecane.

in Fig. 5. For the shell, peaks at 778 and 1050  $\text{cm}^{-1}$  are ascribed to the bending vibration of Si-O-Si.<sup>[27]</sup> The peak at around 3400  $\text{cm}^{-1}$  belongs to stretching vibration and bending



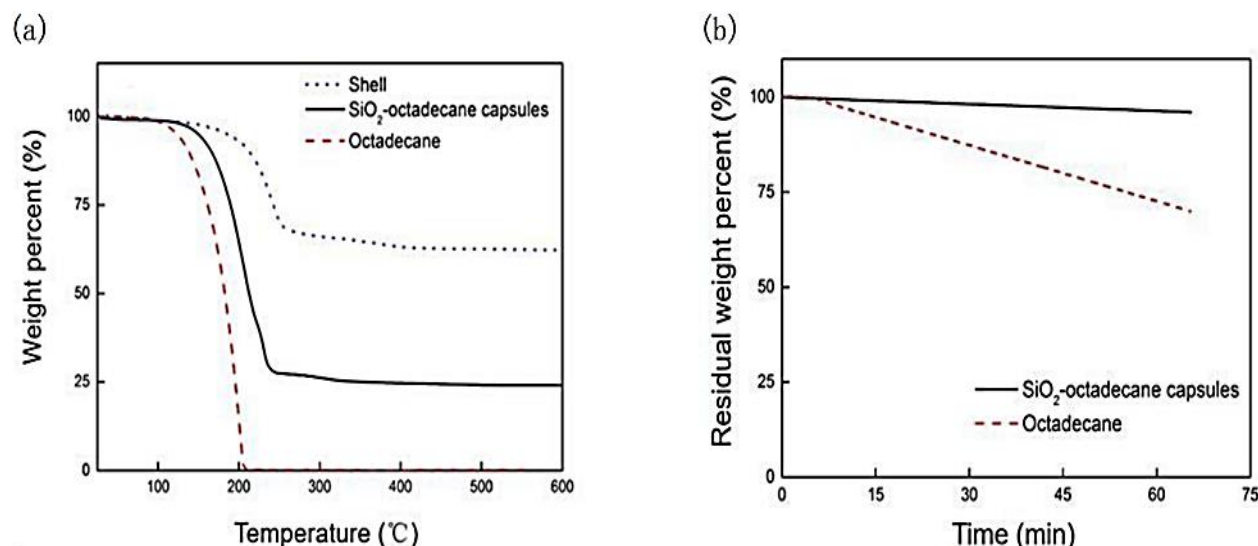


**Fig. 6** (a) TGA curves of shell, SiO<sub>2</sub>-PCM capsules, and octadecane at a heating rate of 10 °C/min in N<sub>2</sub> environment; and (b) isothermal performance of pure SiO<sub>2</sub>-PCM capsules and octadecane heated at 80 °C for 1h.

vibration of functional group of OH.<sup>[28]</sup> Peaks at 1584 and 1626 cm<sup>-1</sup> can be assigned to bending vibration of NH<sub>2</sub>, which is an indicative of the existence of polyurea monomer.<sup>[14]</sup> Moreover, peaks at 1376, 2850 and 2915 cm<sup>-1</sup> correspond to the stretching vibration of C-H(CH<sub>3</sub>), the peak at 1458cm<sup>-1</sup> belongs to the deformation vibration of C-C, and the peak at 718 cm<sup>-1</sup> is attributed to the plane rocking vibration of CH<sub>2</sub>.<sup>[28,29]</sup> For the core octadecane, three typical intensive peaks at 1465, 2850 and 2930 cm<sup>-1</sup> are associated with the alkyl C-H stretching vibrations of methylene and methyl groups.<sup>[21,30]</sup> The FTIR spectrum of SiO<sub>2</sub>-PCM capsules seems to be the superposition of shell and the core octadecane spectra. No new peak was observed in the spectrum of SiO<sub>2</sub>-PCM capsules which indicates no chemical interaction between the core material and the shell during synthesis of SiO<sub>2</sub>-PCM capsules.<sup>[31-33]</sup>

The above FTIR characterization can only indicate the success of microencapsulation, but it cannot confirm the integrity of PCM microcapsule and the compactness of the shell material. Therefore, TGA is needed to further test its performance. TGA is mainly used to characterize the thermal decomposition and then judge the quality of the shell material of the microcapsule. Fig. 6a shows the TGA of octadecane, silica shell, and SiO<sub>2</sub>-PCM capsules. As can be seen, octadecane starts to decompose at about 130 °C and is full decomposed at 230 °C. Two degradation stages can be identified in the TGA curve of silica shell, which are attributed to further dehydration and oxidation of methyl group at higher temperature leading to removal of OH group. For SiO<sub>2</sub>-PCM microcapsules, three decomposition steps were observed in the TGA curve. A small weight loss of 5 wt.% before 130 °C is associated with the evaporation of residual water absorbed on the silica surface. Subsequently, a drastically weight loss between 130 °C and 230 °C is attributed to the evaporation and decomposition of core material. Another degradation stage is after decomposition of octadecane and up to 250 °C which is

due to the decomposition of polyurea membrane. At a much higher temperature range of 300 °C -350 °C, a weight loss of about 7 wt.% is attributed to further dehydration from condensation of silica shell at higher temperature. It reveals that the condensation of silanol is not thorough and there is still some silanol with OH groups adsorbed on the surface of microcapsules.<sup>[34]</sup> Fig. 6b shows the isothermal performance of octadecane and SiO<sub>2</sub>-PCM capsules. As can be seen, octadecane loses approximate 31 wt.% of its weight through evaporation at 80 °C for 1h while the SiO<sub>2</sub>-PCM capsules can maintain the weight without significant weight loss (reduce about 3.4 wt.%). The silica shell therefore effectively prevents leakage of core material.

The thermal stability of capsules can also be tested by DSC in addition to TGA. The principle is that the integrity and compactness of the microcapsule shell material can be proved from the side if there is no change in the enthalpy value before and after several DSC cold and hot cycles. Fig. 7a shows the DSC curves of octadecane, PUA-PCM capsules and SiO<sub>2</sub>-PCM capsules. It obviously indicates that PUA-PCM capsules curve shifts seriously comparing with that of octadecane, meaning that PUA-PCM capsules existed hysteresis phenomenon when PCM melting and solidifying occurred. This phenomenon corresponded to the lower thermal conductivity property of polymer shell. In contrast, curve of silica-PCM capsules is relatively higher and narrower as can be seen in Fig. 7a, which indicates silica has a relative higher thermal conductivity. It clearly reveals that curve of SiO<sub>2</sub>-PCM capsules narrows than that of PUA-PCM capsules, indicating high temperature sensitive of silica shell based capsules. In addition, both initial point of melting and solidifying of silica-PCM capsules were prior to those of PUA-PCM capsules octadecane due to the higher thermal conductivity of silica shell. It is universally known that silica thermal conductivity, about 1.296 Wm<sup>-1</sup>k<sup>-1</sup>, is much higher than that of polymer (0.4 Wm<sup>-1</sup>k<sup>-1</sup>).<sup>[35]</sup> Therefore, on the basis



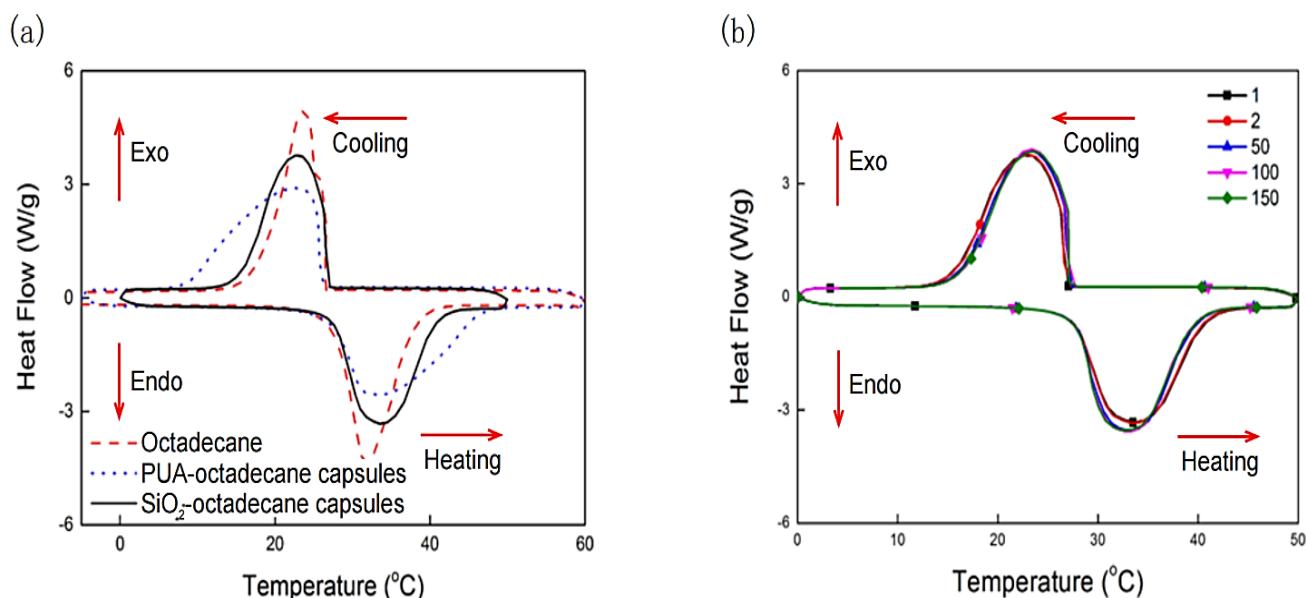


**Fig. 7** (a) DSC process of octadecane, PUA-PCM capsules and SiO<sub>2</sub>-PCM capsules; and (b) DSC melting-solidification cycles of SiO<sub>2</sub>-PCM capsules at a heating rate of 10 °C/min in N<sub>2</sub> environment.

of inorganic silica shell, energy can transfer rapidly between capsules and ambient surrounding during the heating or cooling process, resulting in narrow and high DSC curve.

DSC curves of SiO<sub>2</sub>-PCM microcapsules remain largely unchanged even after 150 heating and cooling cycles (Fig. 7b) suggesting excellent durability and reliability of the capsules. Slight shift of the peak melting and solidification temperatures was observed after a few heating and cooling cycles, which may be attributed to supercooling during phase change. It can be explained as follows. At the first heating-cooling cycle, PCM in microcapsules was solid at the beginning of heating and the portion of PCM touches the internal wall of microcapsules is solid as well. After solidification process, core PCM phase changed to solid again. Nevertheless, the

same portion of PCM contacting internal wall of microcapsules still exists as liquid partially. This phenomenon appears from the second heating-cooling cycle. It reveals that the latter cycle needs relative less heat energy than the former cycle to make core PCM to change from solid to liquid. This specific structure also makes microcapsules response more rapidly and sensitively for heat transfer.

### 3.4 Mechanical strength of SiO<sub>2</sub>-PCM microcapsules

Fig. 8a illustrates a typical compressive load-displacement curve of a single SiO<sub>2</sub>-PCM capsule with a diameter of 300 ± 20 μm (Fig. 6a inset). As can be seen, the compressive load increases gradually in a bi-linear manner. After the peak load, the capsule fractures and softens with a descending of the load

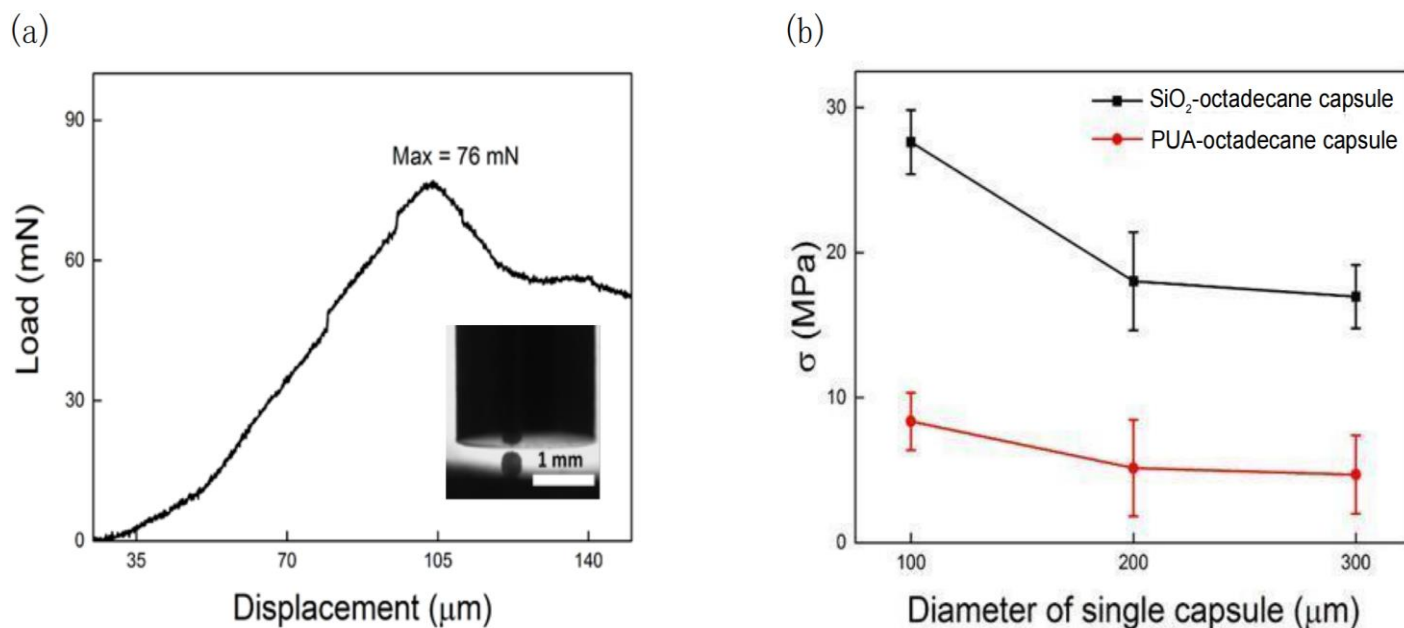


**Fig. 8** (a) Typical compressive load vs. displacement curve of individual SiO<sub>2</sub>-PCM microcapsule with diameter of 300 μm; and (b) compressive strength of microcapsules as a function of capsule size.

carrying capacity. Fig. 8b compares the mechanical strength of single SiO<sub>2</sub>-PCM microcapsule and single PUA-PCM capsule of different sizes. As can be seen, strength of both capsules reduces with increasing size. Similar trend has been reported for other polymer shell capsules.<sup>[36]</sup> Moreover, mechanical strength of SiO<sub>2</sub>-PCM capsules under compression is much higher than that of PUA-PCM capsules (about 3.5 times in current study). Compared to published literature, the strength of 100 µm SiO<sub>2</sub>-PCM capsules in current study reaches 27.6 MPa, which is about 6 times that of a polyurethane microcapsule (4.7 MPa) with the same diameter.<sup>[23]</sup> and higher than that of a hollow glass bubble (12.5 ± 2.0 MPa) with a smaller diameter of around 70 µm.<sup>[37]</sup> The dense inorganic silica shell greatly enhances the mechanical strength of SiO<sub>2</sub>-PCM microcapsules.

#### 4. Conclusion

SiO<sub>2</sub>-PCM microcapsules were fabricated successfully via interfacial polymerization and electrostatic interaction. The resultant microcapsules were characterized through the SEM, TGA DSC, FTIR and compressive strength method. SEM images show that compact and intact silica shell based PCM capsules were obtained, the collected capsules were free-flowing. TGA curves indicates that the final residual weight percentage of capsules was about 20 wt.% after sintered at 600 °C in nitrogen atmosphere. High encapsulation ratio, corresponding to energy storage capacity, about 90 wt.% with capsule diameter 500 µm, was calculated by enthalpy or alternative physical experiment method. Long term performance of silica-PCM capsules investigated via 150 heating-cooling cycles, it showed either initial (1<sup>st</sup> cycle) or final (150<sup>th</sup> cycle) enthalpy of silica-PCM capsules nearly had no changes was ascribed to compact and intact silica shell to inhibit core PCM evaporation and spillage out of capsules. Silica-PCM capsules performed better temperature sensitivity than PUA-PCM capsules due to the high thermal conductivity of silica shell, resulting in the narrow melting and solidification range and high energy storage efficiency. Compression testing indicated that single silica-PCM capsule is robust with a maximum compressive strength (27.6 MPa, size: 100 µm) and much higher than that of polymer shell-based capsule. In conclusion, a facile method to fabricate robust and stable silica-PCM capsules had been developed, silica-PCM capsules probably have the potential commercial applications in energy storage and energy saving.<sup>[38-41]</sup>

#### Acknowledgement

The work is financially supported from the Agency for Science, Technology and Research (A\*STAR) – Ministry of National Development (MND) Singapore (Grant number: SERC132 176 0014), and Department of Science and Technology of Guangdong Province (Project #: 2019A050516006).

#### Supporting Information

Not Applicable.

#### Conflict of Interest

There is no conflict of interest.

#### References

- P. Verma, Varun, S.K. Singal, *Renew. Sustain. Energy Rev.*, 2008, **12**, 999-1031, doi: 10.1016/j.rser.2006.11.002.
- B. Zalba, *Appl. Therm. Eng.*, 2003, 251-283, doi: 10.1016/S1359-4311(02)00192-8.
- D. Zhou, C. Zhao, Y. Tian, *Appl. Energy*, 2012, **92**, 593-605, doi: 10.1016/j.apenergy.2011.08.025.
- A. Jamekhorshid, S. M. Sadrameli, M. M Farid, *Renew. sustain. Energy Rev.*, 2014, **31**, 531-542, doi: 10.1016/j.rser.2013.12.033.
- V. Raj, V. Antony A. Ramalingam Velraj, *Renew. sustain. Energy Rev.*, 2010, **14**, 2819-2829, doi: 10.1016/j.rser.2010.07.004.
- X. Zhai, X. Wang, T. Wang, R. Wang, *Renew. sustain. Energy Rev.*, 2013, **22**, 108-120, doi: 10.1016/j.rser.2013.02.013.
- Al Shannaq, R.M. M. Farid, *Renew. sustain. Energy Rev.*, 2015, 247-284, doi: 10.1533/9781782420965.2.247.
- M. Delgado, A. Lázaro, J. Mazo, B. Zalba, *Renew. sustain. Energy Rev.*, 2012, **16**, 253-273, doi: 10.1016/j.rser.2011.07.152.
- Khudhair, Amar M.Mohammed M. Farid, *Energ. Convers. Manage.*, 2004, **45**, 263-275, doi: 10.1016/S0196-8904(03)00131-6.
- F. Kuznik, K. Johannes, D. David, *Adv. Therm. Energy Storage Syst.*, 2015, 325-353, doi: 10.1533/9781782420965.2.325.
- P. Zhang, Z. W. Ma, R. Z. Wang, *Renew. Sustain. Energy Rev.*, 2010, **14**, 598-614, doi: 10.1016/j.rser.2009.08.015.
- Lei, Jiawei, J. Yang, E. Yang, *Appl. Energy*, 2016, **162**, 207-217, doi: 10.1016/j.apenergy.2015.10.031.
- C. Fan, X. Zhou, *Polym. Bull.*, 2011, **67**, 15-27, doi: 10.1007/s00289-010-0355-1.
- Brown, E. N., M. R. Kessler, N. R. Sottos, S. R. White, *J Microencapsul.*, 2003, **20**, 719-730, doi: 10.1080/0265204031000154160.
- Y. Zhu, B. Huang, J. Wu, *Appl. Energy*, 2014, **132**, 543-550, doi: 10.1016/j.apenergy.2014.06.058.
- H. Zhang, X. Wang, *Sol. Energ. Mater. Sol. C.*, 2009, **93**, 1366-1376, doi: 10.1016/j.solmat.2009.02.021.
- W. Li, X. Zhang, X. Wang, J. Niu, *Mater. Chem. Phys.*, 2007, **106**, 437-442, doi: 10.1016/j.matchemphys.2007.06.030.
- Y. Zhao, Y. Li, D. E. Demco, X. Zhu, M. Moller, *Langmuir*, 2014, **30**, 4253-4261, doi: 10.1021/la500311y.
- C. C. Chang, Y. L. Tsai, J. J. Chiu, H. Chen, *J. Appl. Polym. Sci.*, 2009, **112**, 1850-1857, doi: 10.1002/app.29742.
- A. Zhao, J. An, J. Yang, E. Yang, *Appl. Energy*, 2018, **215**, 468-478, doi: 10.1016/j.apenergy.2018.02.057.
- F. He, X. Wang, D. Wu, *Energy*, 2014, **67**, 223-233, doi: 10.1016/j.energy.2013.11.088.
- G. Fang, L. Hui, F. Yang, X. Liu, S. Wu, *Chem. Eng. J.*, 2009, **153**, 217-221, doi: 10.1016/j.cej.2009.06.019.
- J. Yang, M. W. Keller, J. S. Moore, S. R. White, N. R. Sottos, *Macromolecules*, 2008, **41**, 9650-9655, doi: 10.1021/ma801718v.
- L. Y. Wang, P. Tsai, Y. Yang, *J. Microencapsul.*, 2006, **23**, 3-14, doi: 10.1080/02652040500286045.

- [25] K. Kumarasamy, J. An, J. Yang, E. H. Yang, *Energy*, 2017, **132**, 31-40, doi: 10.1016/j.energy.2017.05.054.
- [26] Z. Jin, Y. Wang, J. Liu, Z. Yang, *Polymer*, 2008, **49**, 2903-2910, doi: 10.1016/j.polymer.2008.04.030.
- [27] Z. Chen, L. Cao, G. Fang, F. Shan, *Nanoscale Microsc. Therm.*, 2013, **17**, 112-123, doi: 10.1080/15567265.2012.761305.
- [28] G. Fang, H. Li, Z. Chen, X. Liu, *J. Hazard. Mater.*, 2010, **181**, 1004-1009, doi: 10.1016/j.jhazmat.2010.05.114.
- [29] H. Zhang, S. Sun, X. Wang, D. Wu, *Colloid. Surface. A*, 2011, **389**, 104-117, doi: 10.1016/j.colsurfa.2011.08.043.
- [30] W. Wang, X. Yang, Y. Fang, J. Ding, *Appl. Energy*, 2009, **86**, 170-174, doi: 10.1016/j.apenergy.2007.12.003.
- [31] M. Destribats, V. Schmitt, R. Backov, *Langmuir*, 2010, **26**, 1734-1742, doi: 10.1021/la902828q.
- [32] S. Yu, X. Wang, D. Wu, *Appl. Energy*, 2014, **114**, 632-643, doi: 10.1016/j.apenergy.2013.10.029.
- [33] T. Toyoda, R. Narisada, H. Suzuki, R. Hidema, Y. Komoda, *Chem. Lett.*, 2014, **43**, 820-821, doi: 10.1246/cl.140099.
- [34] H. Zhang, J. Wu, L. Zhou, D. Zhang, L. Qi, *Langmuir*, 2006, **23**, 1107-1113, doi: 10.1021/la062542l.
- [35] H. Zhang, X. Wang, D. Wu, *J. Colloid Interf. Sci.*, 2010, **343**, 246-255, doi: 10.1016/j.jcis.2009.11.036.
- [36] M. Keller, M. Wade, N. R. Sottos, *Exp. Mech.*, 2006, **46**, 725-733, doi: 10.1007/s11340-006-9659-3.
- [37] H. Zhang, P. Wang, J. Yang, *Compos. Sci. Technol.*, 2014, **94**, 23-29, doi: 10.1016/j.compscitech.2014.01.009.
- [38] X. Lu, H. Liu, V. Murugadoss, I. Seok, J. Huang, J. E. Ryu and Z. Guo, *Eng. Sci.*, 2020, **9**, 25-34, doi: 10.30919/es8d901.
- [39] Y. Zhou, S. Wu, Y. Ma, H. Zhang, X. Zeng, F. Wu, F. Liu, J. E. Ryu and Z. Guo, *ES Energy Environ.*, 2020, **9**, 28-40, doi: 10.30919/esee8c150.
- [40] W. Liao, A. Kumar, K. Khayat and H. Ma, *ES Mater. Manuf.*, 2019, **6**, 49-61, doi: 10.30919/esmm5f606.
- [41] J. Shi, X. Huang, H. Guo, X. Shan, Z. Xu, X. Zhao, Z. Sun, W. Aftab, C. Qu, R. Yao and R. Zou, *ES Energy Environ.*, 2020, **8**, 21-28, doi: 10.30919/esee8c380.

## Author information



**An Jinliang**, Associate Professor in School of Civil Engineering, Hebei University of Engineering (HUE), Director of Green Functional Materials Research Institute@HUE. He received Ph.D. in materials science from Nanyang Technological University in 2017, pursued post-doctoral research at the University of Electronic Science and Technology of China from 2017 to 2019, and served as a project officer of the Center of Engineering Materials and Reliability of the Fok Ying Tung Research Institute, Hong Kong University of Science and Technology, he Joined Hebei University of Engineering in 2019. He Mainly engaged in the research of functional materials such as intelligent temperature control, self-healing, waterproof and anti-corrosion based on microencapsulation technology. In recent years, he has published more than 10 papers in journals such as *Advanced Functional Materials*, *Journal of Materials*

*Chemistry A*, *Energy*, *Applied Energy*, *Energy and Buildings*, and applied for 15 international and domestic patents, including 7 authorized patents.



**Yang En-Hua** is Associate Professor in School of Civil and Environmental Engineering at Nanyang Technological University (NTU), Singapore. Prior to joining NTU, Dr. Yang was Associate in Exponent's Buildings and Structures practice. He received his PhD degree in Civil Engineering from the University of Michigan. Dr. Yang specializes in the development of sustainable infrastructure through the innovative construction materials technology. His principal areas of expertise are fiber reinforced concrete, composite micromechanics, material characterization, and material microstructure analysis and tailoring. He is experienced in the Leadership in Energy and Environmental Design (LEED) green building rating system and is a LEED Accredited Professional certified by the U.S. Green Building Council.



**Duan Fei** joined in Division of Thermal and Fluids Engineering in School of Mechanical and Aerospace Engineering at Nanyang Technological University as an assistant professor on July 11, 2008. Before that, he is a postdoctoral fellow at Thermodynamics and Kinetics Lab of Department of Mechanical & Industrial Engineering in University of Toronto, Canada after he finished his Ph.D. degree there. He finished his B. Sc. & Eng. on Chemical Engineering and M. Sc. & Eng. on Materials Science and Engineering. The focus of Dr. Duan's doctoral and postdoctoral studies was on thermodynamics, heat transfer, and fluid mechanics. During his doctoral study, he visited Institute of Fluid Mechanics at Friedrich-Alexander-University, Erlangen-Nuremberg, Germany.



**Xiang Yong**, Professor, doctoral supervisor (2017-), deputy secretary-general of the Material Gene Composition Committee of the Chinese Society for Materials Science. He received Master and Ph.D. in Harvard University (2000-2005), Deputy Director of the Zhuhai Branch of the State Key Laboratory of Electronic Thin Films and Integrated Devices (2010-), a former member of the "China Material Genome Project" consulting expert group and major "Key New Material Development and Application" Demonstration expert for the direction of genetic engineering of project materials. At present, he mainly engaged in the research of material genetic engineering, all-solid-state lithium battery, battery intelligent management, etc., and has undertaken the Natural Science Foundation, 863 Program, the Ministry of

Industry and Information Technology, the Ministry of Science and Technology Key Special Projects, etc., with cumulative funding of more than 50 million RMB, and more than 150 papers published Article, more than 200 invention patents have been declared.



**Yang Jinglei**, Associate Professor in Hong Kong University of Science and Technology, his research aims at tackling engineering problems via materials innovation, which interfaces cross-disciplinary areas ranging from chemistry, materials engineering, manufacturing to mechanics. His current interests lie in using data-driven materials genome approach to design and manufacture bioinspired multifunctional composites and structures to address the challenging issues in aerospace, building, and transportation sectors. He has extensive fundamental and applied research experiences in the areas and has completed or has been leading more than 30 projects supported by the government and industrial partners since 2009 in microencapsulation, self-healing materials, self-cleaning nanocoatings, energy-efficient materials, and multifunctional composites, and smart manufacturing, etc.

**Publisher's Note** Engineered Science Publisher remains neutral with regard to jurisdictional claims in published maps and institutional affiliations.